ELSEVIER

Journal of Nuclear Materials 264 (1999) 249–256

journal of nuclear materials

Deformation–corrosion interactions for Zr alloys during I-SCC crack initiation
Part II: Localised stress and strain contributions

Patrick Jacques [1], Florence Lefebvre, Clément Lemaignan *

Commissariat à l'Energie Atomique, CEA Grenoble, Service d'Etude du Comportement du Combustible, 17 Rue des Martyrs, F 38054 Grenoble cedex 9, France

Received 4 January 1998; accepted 20 August 1998

Abstract

For a better understanding of the initiation step of iodine induced stress corrosion cracking (SCC) in Zr alloys, responsible for pellet–cladding interaction (PCI) fuel rod failures, an analytical study has been undertaken, the aim of which being focused on the respective roles of local chemistry and stress/strain state on the crack nucleation. This second part is mostly related to the local stress induced by strain incompatibilities between grains. Using EBSP (electron back-scattering pattern) to analyze the crystallographic orientation of all the grains of the samples tested in SCC, it was possible to conclude that the major parameter controlling the nucleation of the intergranular cracks is not related to grain to grain strain incompatibilities, but to the orientation of the grain boundary planes with respect to the tensile stress.

1. Introduction

In water-cooled nuclear reactors, the fuel rod cladding is subject to iodine-induced stress corrosion cracking (SCC) under pellet–cladding interaction (PCI) conditions. The present study is devoted to the crack initiation stage in this failure scheme. The first part compares slow tensile tests performed in inert and iodine-rich atmospheres and shows that crack initiation occurs only in the aggressive environment: crack growth is essentially intergranular and is promoted by local plastic strain. The crack initiation mechanism is therefore primarily of the corrosion–strain interaction type.

Thus, by adsorbing on the surface of the material, iodine may upset the thermochemical equilibrium of the protective film, thereby leading to depassivation of the Zircaloy; however, it seems clear that there is also a mechanical contribution to this depassivation.

This second part of this study deals with the effect of grain orientation in relation to the strain modes of the material. A high degree of heterogeneity of polycrystal strain and a specific plastic behaviour close to the grain boundaries were recorded. In view of this, the impact of grain orientation on crack initiation and microstructural crack location was determined. Finally, the mechanical aspect of these phenomena was analysed.

2. Experimental set-up

The material, test specimen preparation method, experimental apparatus and test procedures have been described in part 1 of this study [1]. Moreover, the crystallographic orientation of the grains was determined using two experimental methods in order to analyse the polycrystalline strains.

To obtain the etching figures, the specimens were electrochemically etched (100 mA cm^{-2}, 250 K, 2 s) in a solution based on that proposed by Kubo [2] (30 g of

* Corresponding author. Tel.: +33-476 88 44 71; fax: +33-476 88 51 51; e-mail: lemaignan@cea.fr.

[1] Present address: EDF SEPTEN, 12 Ave A. Dutrievoz, F 69628 Villeurbanne Cedex, France.

0022-3115/99/$ – see front matter © 1999 Elsevier Science B.V. All rights reserved.
PII: S 0 0 2 2 - 3 1 1 5 (9 8) 0 0 5 0 0 - 5

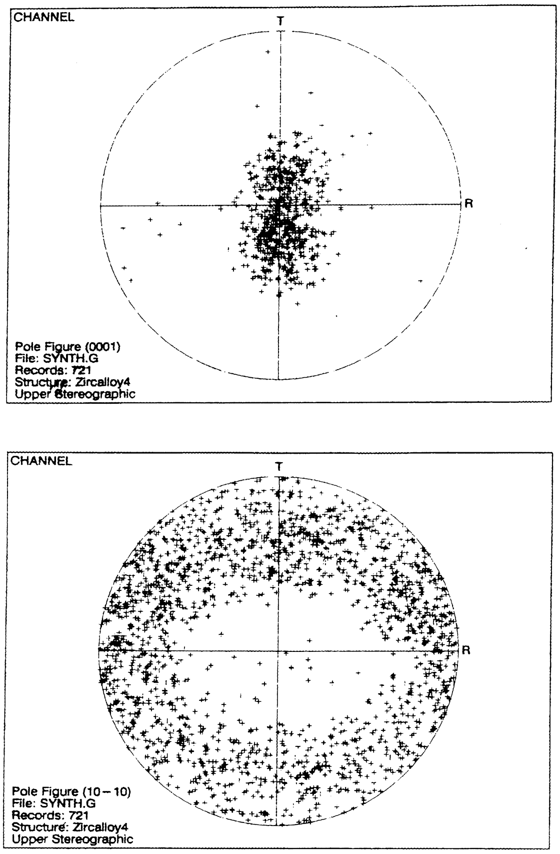

Fig. 1. Discrete pole figure (orientations obtained by EBSP) for all three test specimens.

zinc chloride, 140 g of aluminium chloride, 50 ml of *n*-butyl alcohol and 600 ml of ethanol). While this method gives a good qualitative picture of the crystallographic orientation of the grains, it is nonetheless insufficient for a quantitative approach because of the error induced in the measurement of the angles formed by the sides of the hexagonal prisms of the etch pits.

The second – quantitative – method, EBSP (Electron Back-Scattering Pattern) involves focusing the electrons of an incident beam by families of reticular planes of a crystal [3]. The intensity diagram of the back-scattered electrons, known as pseudo Kikuchi line diagram, is characteristic of the crystalline orientation of the zone swept by the electron beam. With the EBSP method, the electron beam is fixed and the volume of analysed material is typically equivalent to a sphere of 1–2 μm in diameter. The data obtained are processed using a software which determines the changeover from macroscopic reference frame to crystal reference frame.

Normally, the EBSP method requires a material with minimal work-hardening and an unoxidised surface. In practice, usable EBSP pictures can however be obtained from samples with a tensile strain of up to 10%. On the other hand, the absence of any oxide on the surface is an imperative condition. Consequently, it has proved impossible to analyse test specimens tested at 350°C and also to obtain satisfactory indexing of the grains of a specimen tested in iodine-rich methanol. It was for this reason that all the grains on the specimen surface were examined and oriented before tensile testing in an iodine atmosphere. The pole figures reconstructed from EBSP measurements for all three test specimens are given in Fig. 1. By comparing these figures with the conventional pole figure of the material, supplied by Cezus, it was found that the EBSP measurements were statistically reliable.

Three test specimens from the Z2 sheet were therefore indexed by the EBSP method and then subjected to a slow tensile test in an iodine vapour atmosphere, according to the previously described procedure [1]. Specimen No. 3 has the particular feature of having a very large grain (about 700 μm) in the middle of its useful length. Test specimen No. 2 was subjected to a tensile test which was interrupted at 10% and 25%. The characteristics of the three samples are given in Table 1.

All the cracks present at the surface of the three specimens were systematically observed by optical and scanning electron microscopy. A correlation can therefore be established between a crack and the initial crystallographic orientation of the adjacent grains.

3. Results

The observation of the etch figures obtained at the surface of the specimens tested in methanol containing 3×10^{-6} ppm of iodine showed, qualitatively, that crack initiation occurs as well between grains of similar orientations, as between grains of very different orientations (Fig. 2).

Calculations made by means of an auto-coherent model based on the inclusion concept (with variations

Table 1
Crystallographic and cracking information obtained on the samples studied

	Number of indexed grains	Number of pairs of grains	Maximum local strain (%)	Number of cracks detected
Specimen No. 1	321	886	48	24
Specimen No. 2	234	658	40	6
Specimen No. 3	99	259	56	4
Total	654	1803		34

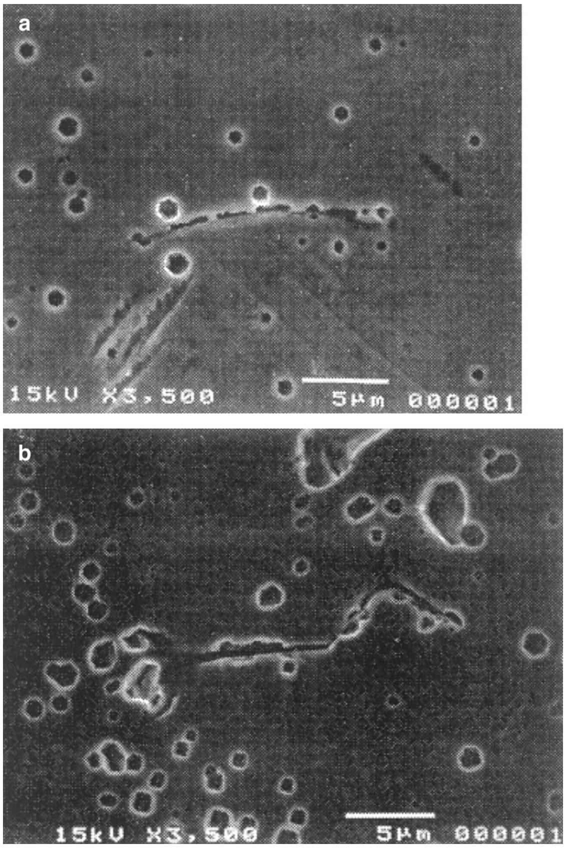

Fig. 2. Localised cracks between grains of similar crystallographic orientations (Z2, iodine-rich methanol, 3 ppm).

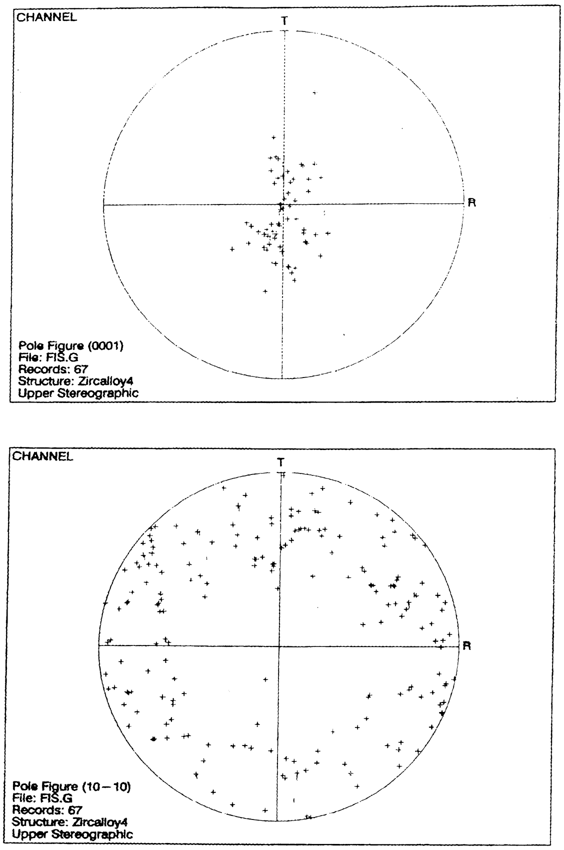

Fig. 3. Discrete pole figures of all the grains in the vicinity of crack initiations observed at the surface of the specimens tested in an iodine vapour atmosphere at 350°C.

on Hill's approximated solution) have proved that the elastic microscopic stresses generated within the polycrystal, by anisotropy of the elastic constants of Zr, are 5% lower than the value of the applied macroscopic stress. It therefore seems necessary to develop an approach based on local plastic strain.

Taking a closer look at the only grains which are adjacent to the crack initiations, the first conclusion of the grain orientation study is that the crystallographic orientations of these grains do not have any special feature but form a statistical subset sample of the orientations of all the grains of each specimen (Fig. 3). Thus, it would seem necessary to find criteria bringing into play the pairs of grains C_{ij} close to each crack in order to be able to analyse polycrystalline behaviour.

Three additional local mechanical criteria were studied in order to determine a grain-to-grain strain incompatibility effect that would be responsible for the local stresses leading to crack initiation: the angular disorientation criterion provides an overall approach to the problem by integrating only crystallographic aspects. The simple expression of grain-to-grain incompatibility enables the orientation of the applied stress to be taken into account and the plasticity of the polycrystal to be understood in a simplistic manner. Finally, the orientation of the grain boundary plane with respect to the applied stress is a geometrical criterion suggested by the observation of cracks mainly perpendicular to this macroscopic stress [1]. To quantify the relevance of a criterion, the cumulative frequencies relative to the pairs of grains adjacent to each other are compared to those relative to the pairs of grains adjacent to the cracks.

3.1. Angular disorientation between adjacent grains

For a pair of grains, (i,j) of known orientations, the angular disorientation is defined as the angle θ_{ij} of the rotation R_{ij} needed to change from the grain i lattice to the grain j lattice. Now the orientation of each "i" indexed grain is provided by the transition matrix M_i from the macroscopic reference frame to the grain reference frame. This matrix M_i is itself a rotation matrix by definition of the Euler angles. Consequently, R_{ij} can be written: $R_{ij} = M_i^{-1} M_j$. However, to take into account the hexagonal lattice symmetries, allowance must be made for all the matrices: $R_{ij}S_{r_i}S_{r_j}$, where S_{r_i} is either the rotation matrix of axis **c** and angle $k\pi/3$ with $k \in \{0,1,2,3,4,5\}$ or the rotation matrix of axis **a** and of angle π.

Consequently, a total of 12 matrices must be taken into account each time:

$$R_{ij}R(\mathbf{a},k'\pi)R\left(\mathbf{c},k\frac{\pi}{3}\right) \quad \text{with } k \in \{0,1,2,3,4,5\}$$

and $k' \in \{0,1\}$.

Moreover, the trace of a rotation matrix R of angle θ, is independent of the reference frame in which the matrix is expressed and is equal to $\mathrm{tr}(R) = 1 + 2\cos\theta$. The angular disorientation between grains i and j thus corresponds to the smallest of the 12 angles obtained from the traces of the 12 rotation matrices considered for each pair (i,j). To evaluate this criterion, a reference curve of cumulative frequencies of the angular disorientations θ_d of all the adjacent grains is compared with a similar curve corresponding to the population of pairs C_{ij} associated with cracks alone. In the latter case, all the pairs of grains C_{ij} adjacent to each crack are analyzed as they are likely to be involved in crack initiation, but only the C_{ij} pair providing the largest angle θ_d was considered.

The pairs of curves obtained for each of the three specimens as well as a summary curve of the three test specimens are shown in Fig. 4. Note that, because of the original texture of the material, 90% of the grain pairs are such that θ_d is less than or equal to 40°. The small difference between the distribution of statistical disorientations between grains and those corresponding to the cracks would seem to indicate that the disorientation between grains is not sufficient to explain the localisation of stress–corrosion crack initiation. A closer look will therefore be taken at the intergranular strain compatibilities.

3.2. Variation in strain difference between two neighbouring grains

A linear hardening law is considered in each grain "i":

$$\tau_i = \tau_0 + h\gamma_i, \tag{1}$$

where τ_i is the resolved stress for grain i relative to the assumed active slipping system, τ_0 the lattice friction stress, h the work hardening coefficient, γ_i the strain of grain i and, in addition, τ_i is defined by:

$$\tau_i = |f_i|\sigma, \tag{2}$$

where σ is the external stress applied and $|f_i|$ is the value of Schmidt factor. From zirconium tensile strain studies, compatible with the emergence of the observed slip lines, a prismatic slipping scheme can be proposed. Of the three possible planes, the one with the largest Schmidt factor is considered.

The local strain becomes:

$$\gamma_i = |f_i|\frac{\sigma}{h} - \frac{\tau_0}{h}. \tag{3}$$

Now the resolved stresses on the most favourable prismatic planes of two neighbouring grains may be equal

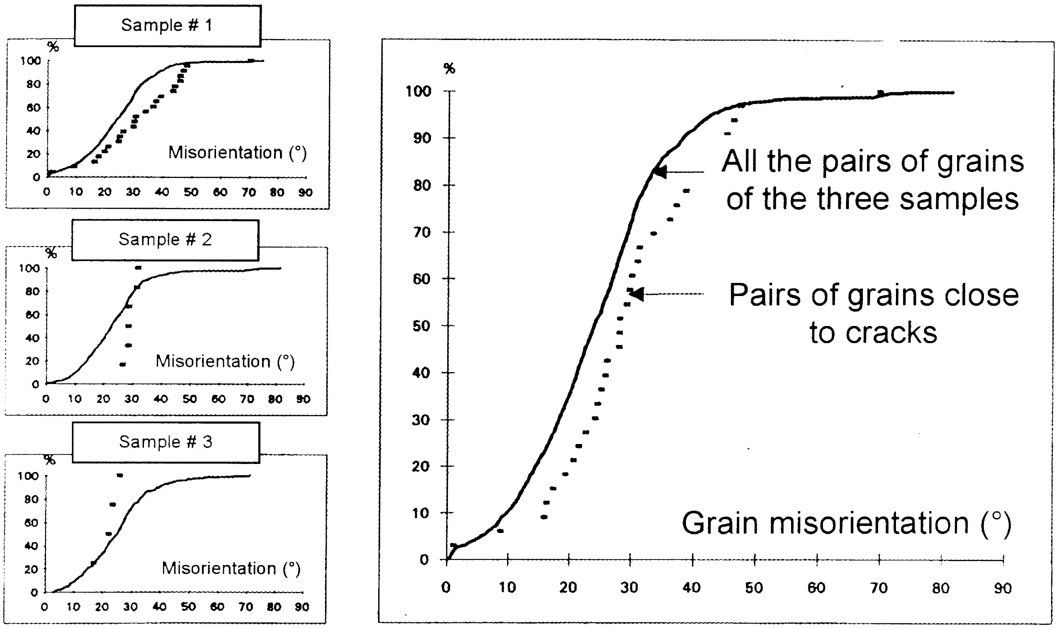

Fig. 4. Cumulative distribution of angular disorientations for pairs of adjacent grains.

without the resulting strain of these grains necessarily being compatible. The vector quantity, $\boldsymbol{\gamma}_i$, is therefore used where the strain direction is given by that of $\mathbf{b}_i$ (Bürgers vector for the prismatic slipping system considered) and the sense by the sign of Schmidt's factor (written $\mathrm{sgn}(f_i)$).

$$\boldsymbol{\gamma}_i = \mathrm{sgn}(f_i)\gamma_i \frac{\mathbf{b}_i}{\|\mathbf{b}_i\|}. \tag{4}$$

Since the norm of Bürgers' vector is independent of the activated prismatic slipping direction and thus independent of the grain i, $\|\mathbf{b}_i\| = b$.

The local oriented strain therefore becomes:

$$\boldsymbol{\gamma}_i = \frac{1}{hb}(\mathrm{sgn}(f_i)\sigma\,|f_i\,|\mathbf{b}_i - \mathrm{sgn}(f_i)\tau_0\mathbf{b}_i). \tag{5}$$

For two neighbouring grains i and j, the quantity:

$$\boldsymbol{\gamma}_{ij} = \boldsymbol{\gamma}_i - \boldsymbol{\gamma}_j \tag{6}$$

represents an expression of incompatibility of strain between the two grains considered. The following relation is obtained:

$$\boldsymbol{\gamma}_{ij} = \frac{1}{hb}\left[\sigma\left(\mathrm{sgn}(f_i)|f_i|\mathbf{b}_i - \mathrm{sgn}(f_j)|f_j|\mathbf{b}_j\right)\right.$$
$$\left. -\tau_0\left(\mathrm{sgn}(f_i)\mathbf{b}_i - \mathrm{sgn}(f_j)\mathbf{b}_j\right)\right]. \tag{7}$$

The norm of this vector, written γ_{ij}, is used to compare the strain incompatibility of different pairs of grains C_{ij}.

The same representation as for the previous criterion is considered. The reference curve representative of the entire population of pairs of neighbouring grains and the curve corresponding to the population of the pairs of grains associated with cracks, are plotted in Fig. 5. Only the distributions concerning test specimens 2 and especially 3 show a major difference between the population of cracks and the reference population, with the points associated with cracks corresponding mostly to high values of the criterion. Without being absolutely discriminating, the grain-to-grain strain incompatibility would appear to promote SCC, only marginally.

3.3. Effect of grain boundary plane trace orientation

Based on an evaluation of the boundary plane opening stress, the third analysis relates to the orientation of the boundary plane trace with respect to the stress axis. Since a comprehensive analysis of all trace orientations would take too long, this problem was approximated by assimilating the trace of a grain boundary to the mid-perpendicular of the segment linking the centres of the grains concerned. For test specimen no. 2, the coordinates of these grain centres were recorded by means of a digitizing table and photographs. The reference curve obtained is practically a straight line (Fig. 6). The distribution of the grain plane trace angle (with respect to the applied stress) is therefore equiprobable in [0, π/2]. Such a result is consistent with the recrystallised state of this metal sheet with equiaxial grains. The equi-probability of boundary trace distribution was therefore assumed to be true and used as a

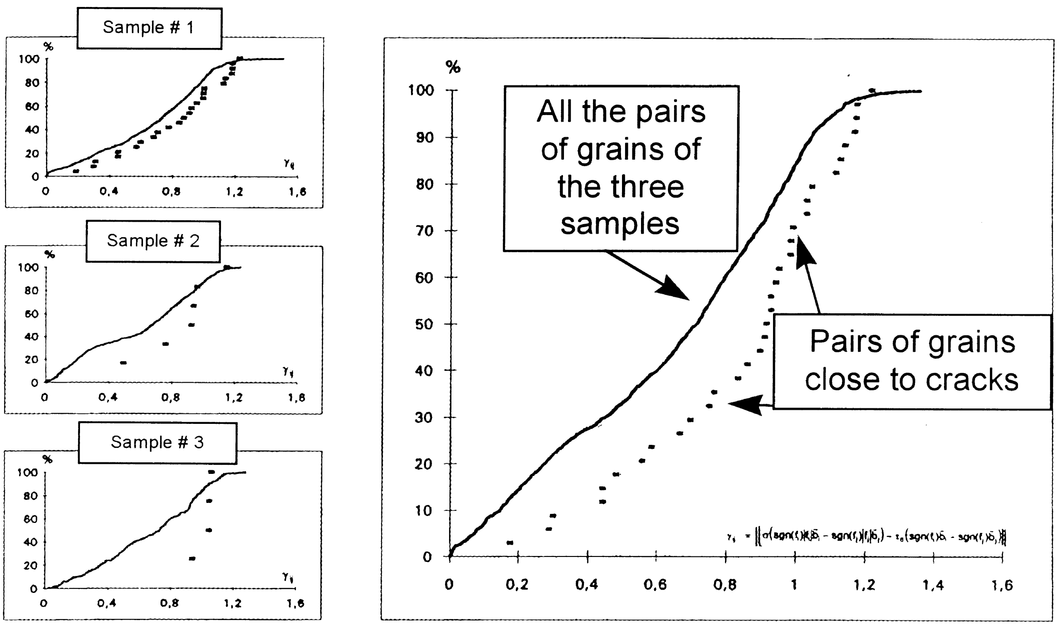

Fig. 5. Effect of strain incompatibility for pairs of grains located at the specimen surface.

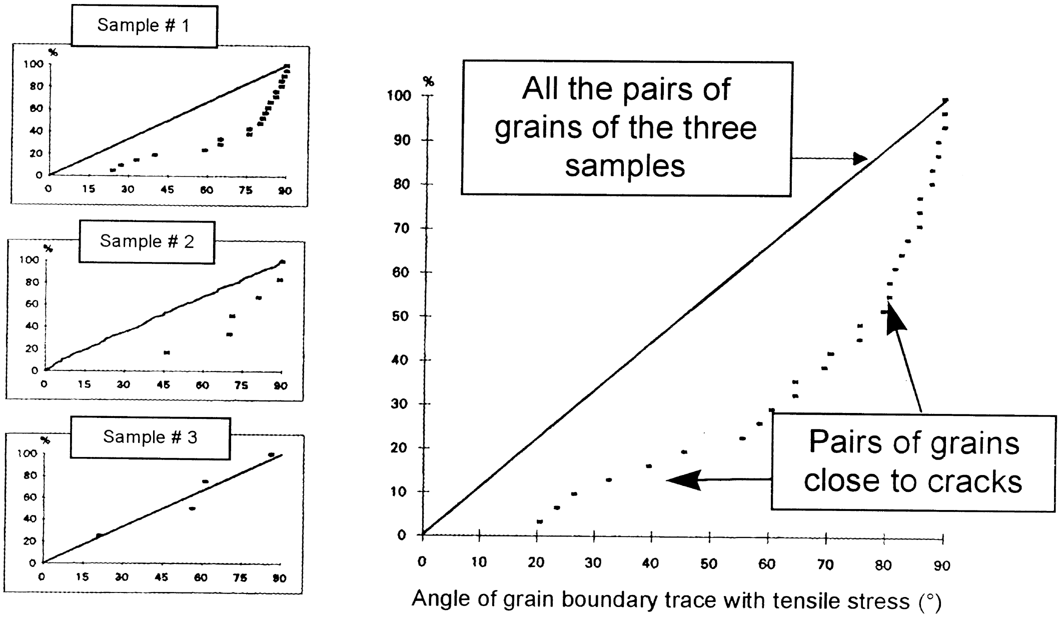

Fig. 6. Distribution of grain boundary trace angle with applied stress.

reference state. The individual measurement of orientation of cracks observed on the samples is superimposed on the reference distributions in Fig. 6. It is clear that, except for test specimen 3 with very few cracks, the probability of crack formation is significantly higher when the trace of the grain boundary plane forms an angle close to 90° with the applied stress. Of the three criteria examined, this is the most discriminating criterion.

4. Discussion

4.1. Influence of strain incompatibilities

At this point, it is perhaps important to give a reminder of certain observations presented in part one: the activation of additional slip systems close to grain boundaries, the appearance of cross slip (at 350°C), especially in the vicinity of triple grain boundaries, as well as the possible occurrence of grain boundary sliding (at 350°C). In classic situations, grain boundary sliding occurs only for temperatures greater than 0.4 T_F but, for the case of zirconium, it appears at relatively low temperature [4]. This could be a contributing factor to the relaxation of the local stresses induced by strain incompatibilities.

However, grain-to-grain strain incompatibilities may be the cause of initiation of intergranular decohesions, as already demonstrated for aluminium–lithium alloys [5]. Even so, the initiation of such cracks cannot be put down solely to the tensile component normal to the boundary plane. This is supported by an elasto-plastic approach made for the simple case of a planar interface, which showed that grain-to-grain strain incompatibilities do not give rise to microscopic stresses perpendicular to the grain boundaries; this result could be extrapolated to the case of polycrystals. It would therefore seem that the cracks resulting from strain incompatibilities would be produced in modes II or III at first, for which stress amplification is possible, with the macroscopic stress subsequently possibly playing a role in providing a mode I opening component.

In a recent study, Kubo [2] suggests that strain incompatibilities are responsible for the initiation of stress corrosion cracks. Being mostly intergranular, these cracks occur preferentially between two grains, only one of which has wide surface slip bands. By measuring the crystallographic orientation of a certain number of grains by etch pits, Kubo proposes a correlation between the existence of intergranular cracks and a high degree of angular disorientation of the adjacent grains (grain-to-grain angle difference of $(\langle C\rangle,\sigma_{\text{applied}})$).

These results could not be confirmed from the observations made thanks to etch pits because many cracks are initiated between two highly deformed grains. As regards the impact of disorientation between grains, the following parameters were taken into consideration:

- The angular disorientation distribution for 1803 pairs of grains compared to that of 34 cracks observed.

This parameter is frequently used in studies of grain boundaries. It is an overall parameter and not simply governed by mechanical effects linked to strain incompatibilities.
- The strain differences between two neighbouring grains take into account, in particular, the case of two adjacent grains with opposing strains, creating a resultant shear stress at the boundary; this situation can lead to mode II or mode III intergranular decohesion followed by opening under normal tensile stress.

In addition, even in the case of samples with little cracking, with regard to angular disorientation, the surface cracks observed correspond to pairs of grains that are not statistically discernible from other pairs.

It can thus be concluded that the cracks are not associated with the pairs of grains corresponding to a maximum for the criteria and, more particularly, that with the criteria proposed, it is not possible to make a clear discrimination between the reference population and the population associated with cracks. However, the representative points of the cracks are slightly distinct from the reference curve. It would therefore seem that the strain incompatibilities, as estimated here, occur upon SCC initiation, but only of the second order.

The analysis given above nonetheless has its limits:
- Only pairs of grains were considered whereas the strain incompatibilities are particularly marked at triple grain boundaries. However, the study of triple grains, no doubt of relevance since the cracks develop preferentially at triple grain boundaries, would appear to be quite difficult because there is no simple mathematical formulation available involving three quantities that allows hierarchical analyses to be made from the scalar result.
- Secondly, the grain orientation measured before the tensile tests was used for the calculations. However, it is known that the texture of zirconium sheets is modified during strain by grain rotation, thus tending to reduce plastic strain incompatibilities.
- Finally, only prismatic slipping was considered with no allowance being made for the effective strain value, which was assumed to be derived directly from the value of Schmidt factor. The prismatic slipping system generally provides a good representation of the strain at the heart of the grains, as found in the present study in certain specific cases. However, slipping along first or second order pyramidal planes may be activated for high strain rates [6] or at triple grain boundaries [7]. It would therefore be advisable to check that the prismatic slipping incompatibilities cannot be relieved by other slip systems. Even so, given the poor knowledge of local stress states and critical resolved shear stresses of different systems, interpreting the calculations would be somewhat hazardous.

4.2. Microstructural location of crack initiation

Stress corrosion cracks in Zircaloy initiate mainly in an intergranular manner, regardless of whether the atmosphere is iodine-rich methanol or iodine vapour. By means of an orientation analysis of each grain, this study concentrated on determining the factors promoting crack initiation at such or such a grain boundary. The position of initiation sites appeared to be independent of the crystallographic orientation of the individual grains, the strainability of pairs of adjacent grains and their relative strain modes.

Moreover, the assessment of the angular disorientation criterion does not provide a means of highlighting the specific behaviour of grain boundaries corresponding to precise disorientation values. Generally speaking, grain boundary energy and chemical reactivity are not particularly dependent on the angular disorientation of adjacent grains, except in the case of sub-boundaries and coincidence boundaries. For example, the intergranular attack of stainless steel in a nitric medium or of aluminium bicrystals in pressurised water is more marked for grain boundaries corresponding to precise angular disorientations [8]. Similarly, the intergranular corrosion of Fe–Ni–Cr polycrystals is also indicative of a higher susceptibility for angular disorientations between 30° and 40° a fact which has been explained in terms of grain boundary structure [9]. The character of grain boundaries can thus have a governing effect on intergranular corrosion [9], on creep-induced intergranular failure [10] or embrittlement of polycrystals by liquid metals [11]; this approach would not appear to be applicable for the iodine-induced stress corrosion cracking of zirconium in the absence of a correlation between angular disorientation and cracking.

On the other hand, it has been shown that the geometrical orientation of the grain boundary trace has an influence with respect to the applied stress. An orientation close to 90° seems to increase the probability of crack initiation (Fig. 6). However, it would appear necessary to extend the 2D approach made on the boundary trace surface to the real orientation (3D) of the grain boundary planes. This orientation is practically inaccessible from an experimental standpoint because it would be necessary to record the orientation of surface grain boundary traces at two depths from the surface. Apart from providing confirmation of the fact that the real angle between the grain boundary plane and the stress is always less than the external trace angle, the use of such an approach would not appear to be able to provide a more discriminating criterion, especially as the monotonic transition from a 2D to a 3D approach would only strengthen this criterion.

Consequently, the relative orientations of grain boundary planes and macroscopic stress would seem to play a dominant role in determining crack initiation locations. This conventional result also tends to confirm that the microscopic aspects related to polycrystal plasticity and, more exactly, to the grain-to-grain strain incompatibilities, do not have a major impact on the initiation mechanism. While the parameters related to the grain boundary structure would not appear to provide an explanation with respect to SCC initiation, the present study nonetheless reveals a systematic effect of the geometrical distribution of grain boundary planes. It may be of interest to consider the impact of this result in the case of Zircaloy cladding in the stress-relieved state. In this state, the highly elongated grains are parallel to the tube axis. Moreover, the stress resulting from Pellet–Cladding Interaction, is oriented circumferentially. Numerous polycrystalline grain boundary planes are therefore perpendicular to the stress. This configuration could thus be conducive to easier initiation of SCC, a fact that would seem to be confirmed by the comparison of SCC behaviour for different metallurgical states [12].

5. Conclusions

Further to the studies related to the chemical aspect and with a view to assessing the impact of crystallography and local strain on iodine-induced stress–corrosion crack initiation, slow tensile tests were performed under iodine vapour on zirconium test specimens containing grains with crystallographic orientations exhaustively predetermined by means of the EBSP method. The effects of intergranular disorientation and strain incompatibilities were studied. It has been shown that pairs of grains associated with the observed figures form a population which can hardly be distinguished from the reference population. Consequently, the crystallographic orientations of neighbouring grains and thus the nature of the grain boundaries would not appear to play a major role in the crack initiation mechanism. Moreover, the high microscopic stresses appearing as a result of strain incompatibilities are no doubt also of second-order importance in the mechanism. It would nonetheless be of interest to be able to generalise the reasoning by taking into account other deformation systems such as the pyramidal or basal systems.

From another standpoint, this study has shown that macroscopic tensile stress and local strains play a dominant role in the crack initiation stage while the geometrical orientation of the grain boundary planes with respect to this tensile stress is the main parameter for explaining the location of iodine-induced stress–corrosion crack initiation sites. The physico-chemical mechanism leading to crack initiation, mainly intergranular from the observations made, still remains unclear. While the orientation of the grain boundary plane with respect to the applied macroscopic stress provides a major criterion for microstructural location of crack initiation, the exact nature of the chemical reactions leading to intergranular embrittlement (by localised oxidation or corrosion) nevertheless requires clarification.

Acknowledgements

The authors would like to give their sincere thanks to J. Driver from the Ecole des Mines de Saint-Etienne for his assistance with EBSP, to M. Humbert from the Université de Metz for the elastic stress concentration calculations, and to Professor F. Louchet for the many constructive discussions. They would also like to thank EDF and Framatome, and more particularly N. Waeckel and P. Melin, for the financial support without which this study would not have been possible.

References

[1] P. Jacques, F. Lefebvre, C. Lemaignan, this issue, p. 239.
[2] T. Kubo, Y. Wakashima, H. Imahashi, M. Nagai, J. Nucl. Mater. 132 (1985) 126.
[3] N. Cheneau-Spath, R.Y. Fillit, J.H. Driver, J. Appl. Crystallogr. 27 (1994) 980.
[4] J. Crepin, T. Bretheau, D. Caldemaison, Acta Mater. 44 (1997) 4927.
[5] C. Verdu, J.M. Gentzbittel, R. Fougeres, A microstructural study of intergranular fracture in 8090 Al–Li alloy, in: Fifth International Al–Li Conference, Williamsburg, VA, 1989, pp. 899–908.
[6] P.G. Partridge, Met. Rev. 118 (1968) 169.
[7] O.T. Woo, G.J.C. Carpenter, S.R. McEwen, J. Nucl. Mater. 87 (1979) 70.
[8] C. Vignaud, L. Beaunier, M. Biscondi, J. Phys. IV 51 (1990) 697.
[9] T. Watanabe, Mater Res. Symp. Proc. 122 (1988) 443.
[10] T. Watanabe, Metall. Trans. A 14 (1983) 531.
[11] T. Watanabe, Res. Mechanica 11 (1984) 47.
[12] L. Brunisholz, C. Lemaignan, Iodine induced stress corrosion cracking of Zy fuel cladding: Initiation and growth, Strasbourg, France, ASTM, ASTM STP 939, 1987, pp. 700–716.